Journal of Colloid and Interface Science 574 (2020) 385–392

Contents lists available at ScienceDirect

Journal of Colloid and Interface Science

journal homepage: www.elsevier.com/locate/jcis

Surfactant/biosurfactant mixing: Adsorption of saponin/nonionic surfactant mixtures at the air-water interface

I.M. Tucker [a], A. Burley [a], R.E. Petkova [a], S.L. Hosking [a], R.K. Thomas [b], J. Penfold [b,c,*], P.X. Li [c], K. Ma [c], J.R.P. Webster [c], R. Welbourn [c]

[a] Unilever Research and Development, Port Sunlight Laboratory, Quarry Road East, Bebington, Wirral, UK
[b] Physical and Theoretical Chemistry Laboratory, Oxford University, South Parks Road, Oxford, UK
[c] ISIS Facility, STFC, Rutherford Appleton Laboratory, Chilton, Didcot, OXON, UK

GRAPHICAL ABSTRACT

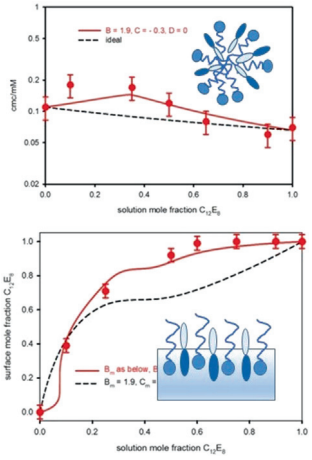

ARTICLE INFO

Article history:
Received 1 April 2020
Revised 15 April 2020
Accepted 15 April 2020
Available online 20 April 2020

Keywords:
Mixed surfactants
Adsorption
Saponins
Escin
Nonionic surfactants
Neutron reflectivity
Air-water interface
Pseudo phase approximation

ABSTRACT

Saponins are naturally occurring biosurfactants present in a wide range of plant species. They are highly surface active glycosides, and are used to stabilise foams and emulsions in foods, beverages and cosmetics. They have great potential for an even wider range of applications, especially when mixed with different synthetic surfactants. Understanding those mixing properties are key to the exploitation of saponins in that wider range of potential applications.

The surface adsorption properties of the saponin, escin, with two conventional nonionic surfactants, polyethylene glycol surfactants, have been studied at the air-water interface using neutron reflectivity, NR, and surface tension, ST.

Although the saponin and polyethylene glycol, C_nEO_m, surfactants are both nonionic the disparity in the relative surface activities and packing constraints result in non-ideal mixing. Comparison with the predictions of the pseudo phase approximation requires the inclusion of the quadratic, cubic and quartic terms in the expansion of the excess free energy of mixing to explain the variations in the surface

* Corresponding author at: ISIS Facility, STFC, Rutherford Aplleton Laboratory, Chilton, Didcot, OXON, Uk.
E-mail address: jeff.penfold@stfc.ac.uk (J. Penfold).

https://doi.org/10.1016/j.jcis.2020.04.061

composition. For escin/pentaethylene glycol monododecyl ether, $C_{12}EO_5$, the interaction is attractive and close to ideal. For escin/octaethylene glycol monododecyl ether, $C_{12}EO_8$, it is repulsive and close to the criteria for demixing. The differences in mixing behaviour are attributed to greater packing constraints imposed by the larger ethylene oxide headgroup of the $C_{12}EO_8$ compared to $C_{12}EO_5$.

1. Introduction

Saponins are a class of biosurfactants which are present in a wide range of plant species [1–5]. These highly surface active glycosides have molecular structures which are quite different to most synthetic surfactants and many other biosurfactants. The hydrophobic part of the molecule consists of a triterpenoid, steroid or steroid-alkaloid group and the hydrophilic region consists of different saccharide residues, which are attached to the hydrophobic scaffold by glycoside bonds. A wide range of different molecular structures are found within the different plant species, and these give rise to a rich variety in their physicochemical properties and biological function and activity.

The intrinsic high surface activity of saponins is the reason for their traditional use as an emulsifier and foam stabiliser in foods [5,6] and beverages [7]. Saponins also exhibit a range of biological properties, and possess anti-inflamatory, anti-fungal, anti-bacterial, anti-cancer, anti-viral and cholersterol lowering functions. This has resulted in applications in natural medicines [8,9], and more recently in cosmetics, shampoos and conditioners and in anti-ageing products [10,11].

The unusual molecular structure of the saponins results in some unusual surface properties, in addition to their high surface activity. The adsorbed surface layers exhibit viscoelastic behaviour, and have very high viscosities and elasticity under dilational and shear forces [12–15]. The unusual surface rheological properties are attributed to the tight molecular packing at the interface and strong hydrogen bonding between neighbouring saccharide groups in the interfacial layer. Recent adsorption measurements and measurements of the surface structure using NR largely confirm this hypothesis [16], and are further supported by recent molecular dynamics calculations [17].

The unusual surface properties and molecular structures of the saponins have given rise to extensive surface studies of saponin adsorption [12–19], and studies of saponin/surfactant [20–22] and saponin/protein mixed adsorption [23–26]. Broadly the saponin/protein mixed adsorption behaviour is similar to that observed in protein/surfactant mixtures [27]. That is at low surfactant concentrations co-adsorption occurs and at high surfactant concentrations the protein is displaced from the surface. However specific interactions between saponin and protein can result in a more complex surface behaviour [23]. Jian et al [20] reported the synergistic lowering of surface tension, ST, and critical micelle concentration, cmc, in saponin/ionic surfactant mixtures, sodium dodecyl sulfate, SDS, and cetyltrimethyl ammonium bromide, CTAB, but not for the nonionic polyoxyethylene surfactant, Brij35. This was largely attributed to the saponin acting as a nonionic component in the mixture and reducing headgroup interactions to produce non-ideal mixing.

In recent years surfactant mixing and the departure from ideality has been extensively studied [28]. It has been demonstrated that NR is a particularly powerful tool for investigating surfactant mixing at interfaces, where adsorbed amounts and the surface composition can be determined directly over a wide range of surfactant concentrations, from below to above the cmc [29]. This approach has provided a more detailed description of surface mixing than is accessible by other techniques, such as ST, and has highlighted the shortcomings of the symmetrical regular solution approach to non-ideal mixing when there are significant electrostatic inter-headgroup interactions present or there is a significant difference or disparity in packing criteria and surfactant structure [30]. In particular it has provided an experimental basis for the validation of the incorporation of higher order terms in the expansion of the free energy of mixing in the pseudo phase approximation approach to non-ideal mixing [31], and it has shown that the analysis of the combination of cmc data and surface compositions provides a more detailed and rigorous approach [31–33]. Even for nonionic mixtures such as triethylene glycol monododecyl ether/octaethylene glycol monododecyl ether, $C_{12}EO_3/C_{12}EO_8$ [32] and nominally nonionic mixtures such as the rhamnolipids L-α-rhamnopyranosyl-β-hydroxydeacnoyl-β-hydroxydecanoate/2-O-α-L-rhamnopyranosyl-α-L-rhamnopyranosyl-β-hydroxyldecanoyl-β-hydroxdeacnoate, R1/R2 [33], significant departures from ideal mixing can occur due to disparities in the packing constraints associated with significant differences in the surfactant structures.

The surface mixing of saponin with conventional synthetic surfactants is expected to be non-ideal due to the unusual molecular structure of the saponins. This was recently demonstrated in the surface mixing associated with the saponin escin and the anionic surfactant SDS [34]. The focus of this paper in the surface mixing of the saponin escin with a range of polyethylene glycol nonionic surfactants, $C_{12}EO_n$, where the structure and relative surface activity of the nonionic surfactant is varied with two different degrees of ethoxylation, n, EO_5 and EO_8.

The saponins offer great potential for a wider range of applications involving biosurfactants, and a key to that widening portfolio of applications is their mixing with different conventional synthetic surfactants. It is hence important to characterise and understand the mixing behaviour of saponins with different synthetic surfactants, and this paper reports part of a series of studies aimed at understanding the nature of biosurfactant/surfactant mixing.

2. Experimental details

2.1. Surface tension

The surface tension measurements were made using a Kruss K100 maximum pull tensiometer and the deNouy method with a platinum-iridium ring. Measurements were made at 25 °C and the ring was rinsed in high purity water and dried under a Bunsen flame before each measurement. Repeated measurements were made until the variation in surface tension was $\leq$ 0.02 mN/m.

2.2. Neutron reflectivity

The neutron reflectivity measurements were made on the SURF [35] and INTER [36] reflectometers at the ISIS pulsed neutron source. The reflectivity, R (Q), was measured as a function of the wave vector transfer, Q, perpendicular to the surface, where Q is defined as $Q = 4\pi\sin\theta/\lambda$, θ is the grazing angle of incidence, and λ is the neutron wavelength. On SURF the measurements were made at an angle of incidence of 1.5° and a λ range of 0.5 to 6.8 Å to cover a Q range of 0.048 to 0.5 $Å^{-1}$. The measurements were made on INTER at an angle of incidence of 2.3° or at 0.8° and 2.3°, and a λ

range of 0.5 to 15 Å to cover Q ranges of 0.03 to 0.5 and 0.01 to 0.5 $Å^{-1}$ respectively. The reflectivity was normalised to an absolute scale by reference to the direct beam intensity and the reflectivity from a deuterium oxide, D_2O, surface. The measurements were made in sealed Teflon troughs containing ~25 mL of solution at a temperature of 25 °C. The measurements were made on a 5 or 7 position sample changer sequentially and each measurement took ~20 to 30 mins.

The reflectivity from a planar surface is directly related to the refractive index distribution perpendicular to the surface. For neutron reflectivity in the kinematic approximation [29] this is expressed as the modulus of the Fourier transform of the scattering length density distribution, ρ(z), where $\rho(z) = \sum_i b_i n_i(z)$ and $n_i(z)$ is the number density distribution of species i and b_i its coherent scattering length. ρ(z) is formally related to the neutron refractive index [29]. Importantly ρ(z) can be manipulated by D/H isotopic substitution as the b values for H and D are quite different (-3.75×10^{-5} and 6.67×10^{-5} Å respectively).

The measurements reported here were made at the air-water interface, in null reflecting water, nrw; that is, a 92 mol% H_2O/8 mol% D_2O mixture with a scattering length density of zero, the same as the air phase. If the adsorbed surfactant has a scattering length density different to zero then there is a reflected signal that arises only from the adsorbed layer, and this has been well established as a route to study adsorption [29]. Here the alkyl chains of the nonionic surfactants are deuterium labelled to provide that contrast in the scattering length density; whereas escin has a sufficient contrast without the need for deuterium labelling. In the absence of deuterium labelling the nonionic surfactants are closely matched to zero. The corresponding ∑b values for the different components used are summarised in Table 1.

The adsorbed layer of surfactant can be adequately described as a monolayer of uniform composition [29] and the reflectivity is then expressed as,

$$R(Q) = \frac{16\pi^2}{Q^2}(2\rho)^2 \sin(Qd/2)^2 \quad (1)$$

where d and ρ are the thickness and scattering length density of the adsorbed layer. For a single adsorbed species the area/molecule, A, and the adsorbed amount, Γ, is related directly to the product d.ρ and ∑b (see Table 1).

$$\Gamma = 1/\mathrm{NaA}, \quad A = \sum b/d.\rho \quad (2)$$

and Na is Avogadro's number.

For a binary mixture A is given by,

$$d.\rho = \sum b_1/A_1 + \sum b_2/A_2 \quad (3)$$

For the escin/nonionic surfactant mixtures studied here two separate reflectivity measurements were made; for escin/h-surfactant, and escin/d-surfactant. The resulting simultaneous equations for the two different d.ρ values can be solved to determine the adsorbed amount of each component at the interface, and this is now a standard approach used for multi-component mixtures [29].

Table 1
∑b values for different surfactant components.

Surfactant species	∑b ($\times 10^{-3}$ Å)
escin	1.78
h-$C_{12}EO_5$	0.09
d-$C_{12}EO_5$	2.70
h-$C_{12}EO_8$	0.22
d-$C_{12}EO_8$	2.87

2.3. Materials and measurements made

The structures of the escin and the different nonionic surfactants used are shown in Fig. 1.

The escin used in this study was obtained from Sigma-Aldrich (part no E1378, batch no. BLCV8469V_3). It was 96% pure and was used as received, without further purification. This was the same batch as used in reference [16], where it was shown that that the impact of the impurities was minimal.

The nonionic surfactants, penatethylene glycol monododecyl ether, and octaethylene glycol monododecyl ether are abbreviated as $C_{12}EO_5$, and $C_{12}EO_8$ respectively; and the hydrogeneous and deuterated versions have a prefix h- or d- respectively. The alkyl chain deuterium labelled d-$C_{12}EO_5$ and d-$C_{12}EO_8$ were provided by the ISIS Isotope Facility, and were synthesised and purified as described elsewhere [37]. The hydrogeneous non-ionic surfactants were obtained from Nikkol and used as supplied. The nonionic surfactants all have a purity of >99.9%.

The D_2O was obtained from Sigma Aldrich and used as supplied, and high purity water (Elga Ultrapure) was used throughout. All the glassware and the Teflon troughs used were cleaned in dilute alkali detergent (Decon90) and rinsed in high purity water.

The surface tension measurements, using h-surfactant in H_2O, were made for escin/$C_{12}EO_5$, and escin/$C_{12}EO_8$ mixtures, in order to determine the variation in the mixed cmc with solution composition.

NR measurements were made at a fixed surfactant concentration of 0.3 mM as a function of solution composition for the isotopic combinations of escin/h-surfactant and escin/d-surfactant, for the nonionic surfactants $C_{12}EO_5$, and $C_{12}EO_8$. For the same surfactants and isotopic combinations NR measurements were made at a fixed escin concentration of 0.01 wt% (9×10^{-5} M) and variable nonionic surfactant concentrations in the range 3×10^{-6} to 10^{-3} M; producing a more complex variation in solution concentration and composition. All the measurements were made in 0.1 M NaCl.

3. Results and discussion

3.1. Surface tension

The ST was measured for the escin/nonionic mixtures, for the nonionic surfactants $C_{12}EO_5$, and $C_{12}EO_8$ and the ST data are shown in Fig. S1 in the Supporting Information for escin/$C_{12}EO_n$ for different escin/$C_{12}EO_n$ compositions. The variation in mixed cmc with solution composition for both mixtures is shown in Fig. 2.

Although the cmc of the nonionic surfactants increases from 4.7×10^{-5} M to 7×10^{-5} M as the EO length increases from EO_5 to EO_8 [38], the cmc values for both the nonionic surfactants studied are relatively close to that for escin, 1.1×10^{-4} M [16]. As shown in Fig. 2 the variation in the cmc for both mixtures is relatively close to ideal, and the dashed lines in Fig. 2 are for ideal mixing using the Clint equation [39],

$$\frac{1}{c^{\mu}_{mix}} = \frac{\alpha_1}{c^{\mu}_1} + \frac{\alpha_2}{c^{\mu}_2} \quad (4)$$

where c^{μ}_{mix} is the mixed cmc, α_i and c^{μ}_i are the solution mole fraction and cmc of component i. The solid lines are calculations for non-ideal mixing, using the pseudo phase approximation, see Holland and Rubnigh [40]. In the pseudo phase approximation the components of the pseudo phases, micelles, surface, and solution monomer, have the same chemical potential at equilibrium. Equating the chemical potential of the micelles and monomer [31,39,40] gives,

$$x_i = \frac{c^{mon}_i}{f^m_i c^{\mu}_i} \quad (5)$$

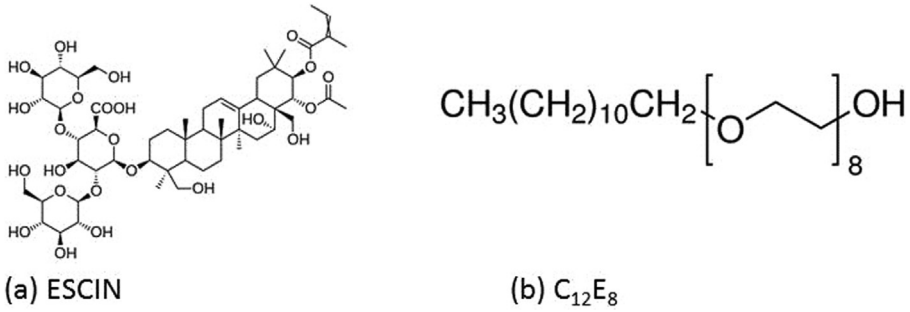

Fig. 1. Structure of surfactant components (a) escin, (b) $C_{12}EO_8$, $C_{12}EO_5$ has a similar structures but with 5 ethylene oxide groups.

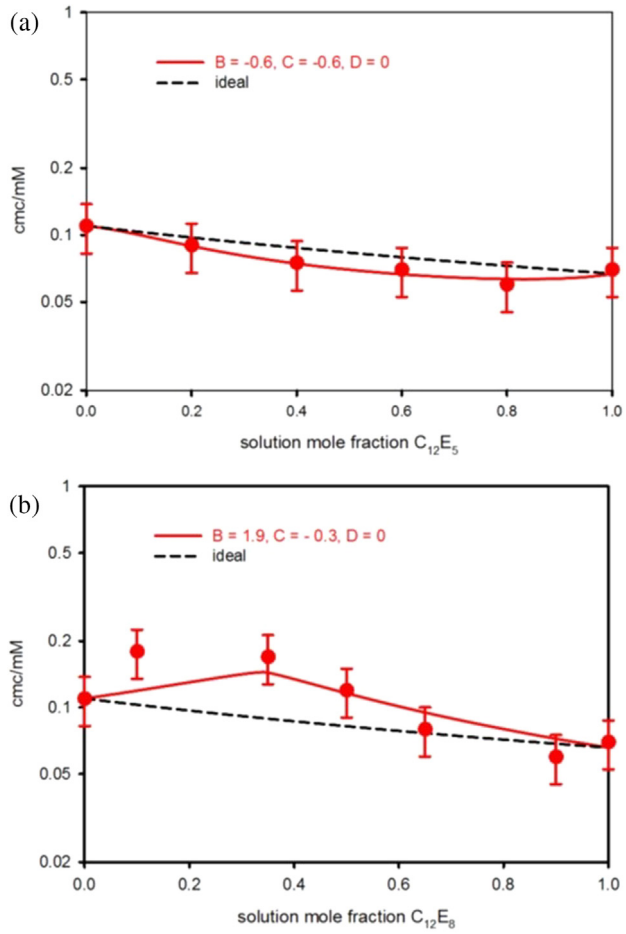

Fig. 2. Variation in cmc with solution composition for escin/nonionic surfactant mixtures, (a) $C_{12}EO_5$, and (b) $C_{12}EO_8$. The dashed and solid lines are for ideal and non-ideal mixing, as described in the main text and for the parameters listed in Table 2, see legend for more details.

where x_i is the mole fraction of the i^{th} component in the micelle, c_i^{mon} the monomer concentration of the i^{th} component, f_i^m its activity coefficient in the micelle, and c_i^{μ} its cmc. For a binary mixture, assuming the micelle mole fractions equal unity and at the cmc $c_i^{mon} = \alpha_i c_i^{mix}$, where α_i is the mole fraction of monomer in solution and c_{mix}^{μ} the mixed cmc,

$$\frac{1}{c_{mix}^{\mu}} = \frac{\alpha_1}{f_1 c_1^{\mu}} + \frac{\alpha_2}{f_2 c_2^{\mu}} \tag{6}$$

Here the activity coefficients are derived from an expansion of the excess free energy of mixing, Ge, which includes quadratic, cubic and quartic terms [28,38–40] such that,

$$Ge = RT[x_1 x_2 B_{12} + x_1 x_2 (x_1 - x_2) C_{12} + x_1 x_2 (x_1 - x_2)^2 D_{12}] \tag{7}$$

where B_{12}, C_{12} and D_{12} are the interaction constants. They are abbreviated to B, C and D in this paper and have the subscripts m and s when referring to the micelle and surface mixing separately. In the Regular Solution approximation C_{12} and D_{12} are zero, and the interaction is symmetrical about the surface or micelle composition. The higher order terms, in particular, account for the asymmetry in the mixing that often occur, especially in ionic/nonionic mixtures [31–34,41–43]. This leads to a set of equations that can be solved interatively to obtain, in addition to the cmc variation, the micelle, surface and monomer compositions above and below the cmc [31,41].

The pseudo phase approximation parameters used to analyse the cmc data in Fig. 2 and the variation in surface composition (see later) simultaneously are summarised in Table 2. It has now been comprehensively demonstrated that determining the variation in surface composition provides a more stringent and sensitive measure of non-ideal mixing in surfactants [29–31,41–43], and in the following section this is pursued using NR.

For escin/$C_{12}EO_5$ the variation of the mixed cmc with composition is close to ideal, and is best described by a slightly attractive interaction between the escin and $C_{12}EO_5$. In contrast the variation in the mixed cmc for escin/$C_{12}EO_8$ shows a pronounced positive deviation from ideality, and is best described by a repulsive interaction between the escin and $C_{12}EO_8$. The values for B and C in that case are close to the condition associated with demixing or phase separation; where values $\geq$2.0 denote demixing. In both cases the inclusion of a finite cubic term (C parameter) implies some asymmetry in the interaction with composition, and is discussed in more detail later in the context of the surface mixing.

3.2. Neutron reflectivity

NR measurements were made for the escin/$C_{12}EO_5$, and escin/$C_{12}EO_8$ mixtures in nrw at a fixed solution concentration of 0.3 mM, and variable solution composition; and for the isotopic combinations escin/h-surfactant, escin/d-surfactant. From the cmc data in Fig. 2, a solution concentration of 0.3 mM is greater than the mixed cmc for both of the mixtures. The NR data were analysed using equations 1–3 and for the $\sum$b values in Table 1, to obtain the adsorbed amount of each component and hence the

Table 2
Non-ideal interaction parameters for micelles (m) and surface (s) for escin/nonionic *surfactant mixtures (in units of RT).*

Mixture	B	C	D
escin/$C_{12}E_5$ (m)	−0.6	−0.6	0.0
escin/$C_{12}E_5$ (s)	−0.5	−0.5	0.0
escin/$C_{12}E_8$ (m)	1.9	−0.3	0.0
escin/$C_{12}E_8$ (s)	1.6	−0.2	1.0

Table 3
d.ρ values for some 0.3 mM escin/$C_{12}EO_8$ mixtures.

Mixture	Composition (mole fraction escin)	d.ρ value (±0.05 x10^{-5} Å^{-2})	
		hh	hd
escin/$C_{12}EO_8$	0.75	1.05	3.95
	0.5	0.55	4.50

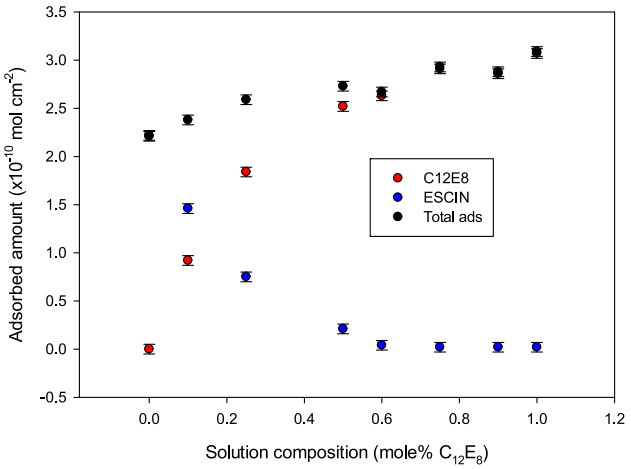

Fig. 3. Adsorbed amount, Γ, ($\times 10^{-10}$ mol cm^{-2}) versus solution composition (mole % nonionic) for escin/$C_{12}EO_8$, (black) total adsorption, (red) nonionic, (blue) escin. (For interpretation of the references to colour in this figure legend, the reader is referred to the web version of this article.)

surface composition. The NR data are well described as a monolayer and modelled using equation [1] to obtain a thickness, d, and scattering length density, ρ. The thickness obtained is typically ~24 ± 4 Å; but as discussed earlier, in terms of determining the adsorbed amount the product d.ρ is the important factor. Some typical d.ρ products are summarised in Table 3 below, and some representative NR data and associated model fits are shown in Fig. S2 in the Supporting Information for 0.3 mM 90/10 mol ratio Escin/$C_{12}EO_8$.

The variations in the adsorbed amounts and total adsorption for 0.3 mM escin/$C_{12}EO_8$ are shown in Fig. 3, and for escin/$C_{12}EO_5$ in Fig. S2 in the Supporting Information. The area/molecule, adsorbed amounts, Γ, total adsorption, and surface composition values are tabulated in Table 4.

The adsorption data for escin/$C_{12}EO_8$ and escin/$C_{12}EO_5$ (see Fig. 3, and Fig. S3 in the Supporting Information, and Table 4) show broadly similar trends. That is, the total adsorption increases as the solution composition varies from escin rich to nonionic rich, reflecting the change in the area/molecule from escin to $C_{12}EO_8$ ($C_{12}EO_5$), see Table 4. As the solution composition changes from escin rich to nonionic rich the relative amounts of the two components at the interface over much of the composition range is dominated by the nonionic adsorption.

As shown in Fig. 4, the variation in the surface composition for escin/$C_{12}EO_5$, and escin/$C_{12}EO_8$ with solution composition show broadly similar trends, and the adsorption is dominated by the nonionic adsorption over much of the composition range.

As measured by their relative cmc's (see Fig. 2), the relative surface activities of escin, $C_{12}EO_5$, and $C_{12}EO_8$ are not significantly different. However the limiting area/molecule of the pure components vary significantly, 40 Å^2 for $C_{12}EO_5$, 54 for $C_{12}EO_8$, and 69 for escin, but these variations do not necessarily reflect variations in surface activity.

The solid line in Fig. 4a is from a pseudo phase approximation calculation, as described earlier, for the variation in surface composition with solution composition for escin/$C_{12}EO_5$, with the B and C parameters (see equation (7)) as summarised in Table 2, and using the same micelle mixing parameters derived from the mixed cmc data. The dashed line is for the same non-ideal micelle mixing, but for ideal mixing at the surface. The dashed and solid lines in Fig. 4a show that the surface mixing is relatively close to ideal. The parameters also indicate only a slight departure from ideal mixing at the surface, and the surface parameters are very similar to the micelle parameters. The inclusion of the cubic term shows that interaction is not symmetrical. However the closeness to ideal mixing shows that the variation in the surface composition and the dominance of the $C_{12}EO_5$ is reflecting the relative surface activity of the two components, and in this case the $C_{12}EO_5$ is more surface active.

Although the variation in the surface composition with solution composition for escin/$C_{12}EO_8$ (see Fig. 4b) has a broadly similar trend to that for escin/$C_{12}EO_5$, in detail it is different and the corresponding surface mixing parameters (see Table 2) are notably different. Furthermore the departure from ideal mixing is greater. The

Table 4
Variation in adsorbed amount and surface composition with solution composition for 0.3 mM escin/nonionic surfactant, (a) escin/$C_{12}EO_8$, (b) escin/$C_{12}EO_5$.

Solution composition (mole ratio $C_{12}EO_8$/escin)	$C_{12}EO_8$		escin		Γ_{total} (±0.05 × 10^{-10} mol cm^{-2})	Surface composition (±–0.02)mole % $C_{12}E_5$)
	A (±5 Å^2)	Γ (±0.05 × 10^{-10} mol cm^{-2})	A (±5 Å^2)	Γ (±0.05 × 10^{-10} mol cm^{-2})		
(a)						
100/0	54	3.07	–	–	3.07	1.0
90/10	58	2.86	–	–	2.86	1.0
75/25	57	2.91	–	–	2.91	1.0
60/40	63	2.63	4050	0.04	2.67	0.99
50/50	66	2.52	795	0.21	2.73	0.92
25/75	90	1.84	220	0.75	2.59	0.71
10/90	181	0.92	114	1.46	2.38	0.39
0/100	–	–	69	2.41	2.41	0.0
(b)						
100/0	40	4.15	–	–	4.15	1.0
95/5	41	4.05	–	–	4.05	1.0
90/10	41	4.05	–	–	4.05	1.0
75/25	41	4.05	–	–	4.05	1.0
50/50	53	3.13	430	0.4	3.53	0.89
25/75	77	2.16	178	0.93	3.09	0.70
0/100	–	–	75	2.21	2.22	0.0

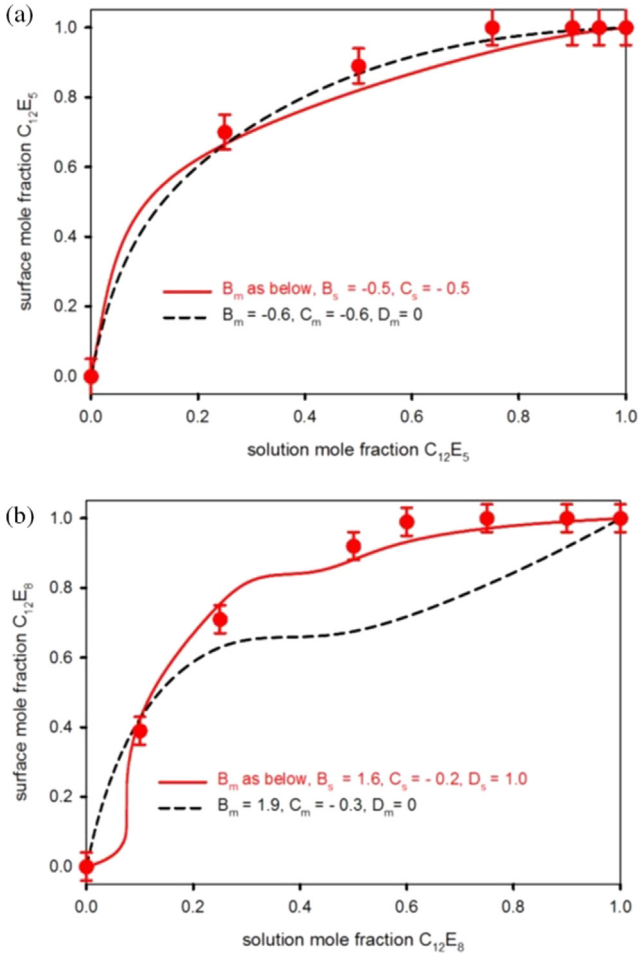

Fig. 4. Variation in surface composition (mole% nonionic) with solution composition (mole% nonionic) for 0.3 mM escin/nonionic, (a) $C_{12}EO_5$, (b) $C_{12}EO_8$. The dashed and solid lines are calculations using the pseudo phase approximation, as described in the text, and in the legend.

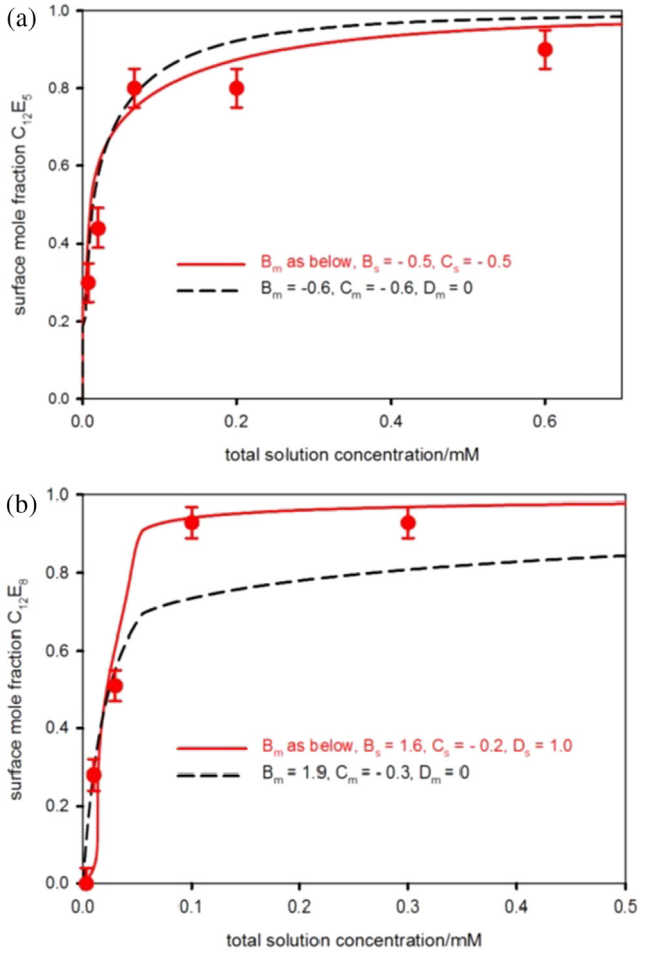

Fig. 5. Variation in surface composition (mole % nonionic) versus surfactant concentration for 0.01 wt% (9×10^{-5} M) escin/Surfactant mixtures, (a) escin/$C_{12}EO_5$, (b) escin/$C_{12}EO_8$. The solid and dashed lines are pseudo phase approximation calculations as described in the text and legend, and using the parameters in Table 2.

dashed line in Fig. 4b assumes ideal mixing at the surface, but non-ideal mixing with a repulsive interaction for the micelle mixing (as derived from the cmc data in Fig. 2). The solid line is for the surface and micelle mixing parameters in Table 2, and which now describes a repulsive interaction. The surface and micelle mixing parameters are similar, except that to fully describe the surface behaviour quadratic, cubic and quartic terms are required in the expansion of the excess free energy of mixing. In both the surface and micelles the parameters indicate a repulsive interaction close to the conditions for demixing, and an asymmetry in the interaction with solution composition.

The differences between the parameters required to describe the escin/$C_{12}EO_5$ and escin/$C_{12}EO_8$ mixing reflect the different packing constraints associated with the larger ethylene oxide headgroup of $C_{12}EO_8$ compared to $C_{12}EO_5$, and is discussed in more detail later in the discussion.

In the context of formulating products it is instructive to evaluate also how the relative adsorption varies at a fixed Saponin concentration and variable surfactant concentrations. Hence NR measurements were also made at a fixed escin concentration of 0.01 wt% (9×10^{-5} M) and variable nonionic surfactant concentrations (for $C_{12}EO_5$, and $C_{12}EO_8$) over a concentration range from 0.003 to 4.0 mM (depending upon the nonionic surfactant). In this case the solution composition and concentration vary simultaneously and a different more complex pattern is followed, which varies from below to above the cmc. Fig. 5 shows the variation in surface composition with solution concentration for escin/$C_{12}EO_5$, and escin/$C_{12}EO_8$, at a fixed escin concentration of 0.01 wt%.

The corresponding variations in the adsorbed amounts are shown in Fig. S4 in the Supporting Information, and key parameters are summarised in Table S1 in the Supporting Information. The parameters in Table S1 show how solution concentration and solution composition vary with the changing nonionic surfactant concentration. Qualitatively the trends observed at a fixed escin concentration and variable nonionic concentration are broadly similar to those at a fixed total concentration and variable solution composition. When the relative compositions and concentrations are taken into account the two data sets are also broadly consistent quantitatively.

The solid and dashed lines in Fig. 5 again correspond to ideal mixing at the surface and non-ideal mixing in the micelles (dashed line), and non-ideal mixing at the surface and in the micelles (solid line). Importantly the pseudo phase approximation calculations were made using same parameters (see Table 2) as obtained from the cmc variation (Fig. 2) and the surface composition variations at a fixed concentration (Fig. 3).

3.3. Discussion

The surface and micelle mixing for escin/$C_{12}EO_5$ is close to ideal and has a slightly attractive interaction; and in which the micelle

mixing is slightly less ideal than the surface. This interaction, as characterised through the pseudo phase approximation, requires both the quadratic and cubic terms in expansion of the excess free energy of mixing. Hence it is asymmetrical about the surface and micelle compositions. The closeness to ideal mixing is consistent with the escin behaving like a nonionic surfactant, as previously reported [16,34]. From NR and ST data in reference [16] it was concluded that escin was only weakly anionic at high pH and behaved over the entire pH range measured, 4 to 8, like a nonionic surfactant. In contrast the surface and micelle mixing for escin/$C_{12}EO_8$ are best described by a repulsive interaction, and are close to the criteria for demixing. In this case the interaction is also asymmetrical about the surface and solution compositions, and the micelle mixing is slightly less ideal than the surface. Furthermore the asymmetry in the surface mixing is such that quadratic, cubic and quartic terms in the expansion of the excess free energy of mixing are required to describe the surface mixing behaviour.

The mixing properties of escin with different conventional surfactants have been studied by Jian et al [20] and Tucker et al [34]. Jian et al [20] reported a synergistic reduction in the mixed cmc for SDS/escin and CTAB/escin, but not for the mixture of escin with the nonionic surfactant Brij35. Tucker et al [34] studied the surface and micelle mixing of SDS/escin mixtures in 0.1 M NaCl by NR and ST. Their analysis using the pseudo phase approximation showed an asymmetrical synergistic attractive interaction, giving rise to a stronger interaction in the micelles than at the surface. The minimum in the free energy of mixing corresponds to a surface mole fraction of SDS ~0.3. This was interpreted, as the measurements were made in 0.1 M NaCl reducing the electrostatic contribution to the interaction, as due to both electrostatic and steric effects.

For escin/$C_{12}EO_5$ the minimum in the excess free energy of mixing, Ge_{min}, is ~ −0.15 RT, and is slightly attractive, but reflecting the closeness to ideal mixing. The surface composition at the free energy minimum corresponds to a surface mole fraction of 0.67 of $C_{12}EO_5$. This ratio, in ionic/nonionic mixtures, is often attributed to the optimal nonionic/ionic mixture of a 2-D ordered array of charged and uncharged species which minimises repulsion. Here, as both the $C_{12}EO_5$ and escin are effectively nonionic, this asymmetry reflects the mismatch in the packing criteria between the two components. For escin/$C_{12}EO_8$ the corresponding maximum in the excess fee energy of mixing in the surface corresponds to a surface mole fraction of $C_{12}EO_8$ ~ 0.43 RT, close to symmetrical. However the mixing parameters (see earlier in Table 2) do not correspond to a regular solution description, and the close to symmetrical value is a coincidence due to competing contributions from the quadratic and cubic terms in the expansion of the excess free energy of mixing. The maximum in the excess free energy of mixing corresponds to a value ~ +0.4 RT; reflecting the larger repulsive interaction between the two components.

The slight departure from ideal mixing for the escin/nonionic surfactant mixtures reported here is consistent with the escin acting effectively as a nonionic surfactant. The attractive interaction between the escin and $C_{12}EO_5$ is consistent with both surfactants having a tendency towards planar structures, and this is particularly well established for $C_{12}EO_5$ [44]. In this case the asymmetry in the interaction between the escin and $C_{12}EO_5$ can be attributed to packing constraints imposed by the different surfactant geometries. $C_{12}EO_8$ has a tendency towards forming small globular micelles and hence a greater preferred curvature [45]. The different packing constraints and preferred curvatures associated with the escin and $C_{12}EO_8$ are then in part responsible for the repulsive interaction between them, in the micelles and at the surface. There is, however, a further factor which may contribute to both the $C_{12}EO_8$ and $C_{12}EO_5$ mixing with escin. This arise from an intrinsic incompatibility between the sugar groups of the escin and the nonionic surfactant ethylene oxide groups, which manifest itself as a weak or unfavourable interaction [46–48], and this may have a greater impact upon the mixing with $C_{12}EO_8$ than with $C_{12}EO_5$.

4. Conclusions

The surface and micelle mixing of the biosurfactant saponin with different nonionic surfactants has been studied using NR and ST. For the two polyethylene glycol surfactants studied, $C_{12}EO_5$ and $C_{12}EO_8$, the mixing is close to ideal. However a detailed analysis of the data provides an indication of the main factors contributing to the non-ideality.

For the escin/$C_{12}EO_5$ mixture the interaction is slightly attractive; whereas for the escin/$C_{12}EO_8$ mixture it is repulsive and close to the conditions for demixing. In both cases the mixing data are analysed using the pseudo phase approximation, in which the inclusion of quadratic, cubic and quartic terms in the expansion of the excess free energy of mixing are required. The asymmetry in the mixing is attributed to the relative packing contraints and preferred curvatures of the different components. Furthermore the weak interaction between the escin sugar groups and the ethylene oxide groups of the non-ionic surfactants is an additional factor, contributing to the weak interaction observed. This later factor and the more extreme packing requirements between escin and $C_{12}EO_8$ are both important contributions to the repulsive interaction between escin and $C_{12}EO_8$.

The close to ideal mixing for the saponin/nonionic surfactant mixtures contrasts with the mixing behaviour of the saponin/ionic surfactant mixtures [20,34], where a strong synergistic attractive interaction occurs. For the saponin/nonionic surfactant mixtures the non-ideality is largely driven by packing constraints, steric contribution, whereas in the saponin/ionic surfactant mixtures there are electrostatic and steric contributions.

The results contribute greatly to the understanding of the interaction of saponins with a range of conventional surfactants, and to the possibility of their wider use in a range of formulations. The study provides a basis for a broader investigation of saponin/surfactant mixing at interfaces and in bulk aggregates.

Declaration of competing interest

The authors declare that they have no known competing financial interests or personal relationships that could have appeared to influence the work reported in this paper.

Acknowledgements

The provision of beam time on the SURF and INTER reflectometers at ISIS is acknowledged. The invaluable scientific and technical assistance of the Instrument Scientists and support staff is greatly appreciated. IMT, AB, REP, and SLH thank Innovate UK for funding under the IB catalyst scheme, grant no. 131168, “A synthetic biology-based approach to engineering triterpenoid saponins and optimisation for industrial applications”.

Author contributions

All the authors have contributed to the different aspects of the paper, which include the experimental design and measurement, interpretation and analysis of the data, preparation and approval/editing of the manuscript, and management of resources; and specifically IMT, AB, REP, RKT, JP , PXL, KM, JRPW and RW have been involved in the measurement and interpretation of the data and experimental design, JRPW and SLH in the management of resources, and IMT, RKT, JP, PXL, JRPW, and SLH in the editing of the manuscript.

Funding Sources

Funded through the beam time awarded at the STFC's ISIS Facility, and funding from Innovate UK under the IB catalyst scheme, grant no. 131168, "A synthetic biology-based approach to engineering triterpenoid saponins and optimisation for industrial applications".

Appendix A. Supplementary material

Supplementary data to this article can be found online at https://doi.org/10.1016/j.jcis.2020.04.061.

References

[1] K. Hoslettman, A. Marston, Saponins, Cambridge University Press, New York, 1995.
[2] O. Guclu-Ustandag, G. Mazza, Spaonins: properties, applications and processing, Crit. Rev. Food Sci. Nutr. 47 (2007) 231–258.
[3] S.G. Sparg, M.E. Light, J. van Staden, Saponins: biological activities and distribution of plant saponins, J. Ethnopharmacol. 94 (2004) 219–242.
[4] J.P. Vinken, L. Heng, A. de Groot, H. Gruppen, Saponins: classification and occurrence in the plant kingdom, Phytochemistry 68 (2007) 275–297.
[5] D. Oakenfull, Saponins in food- a review, Food Chem. 6 (1991) 19–40.
[6] P.R. Cheeke, Actual and potential applications of Yucca Schidigera and Quillaja Saponana saponins in human and animal nutrition, Proc. Am. Soc. Anim. Sci. E9 (1999) 1–10.
[7] S. Bottcher, S. Drusch, Interfacial properties of saponin extracts and their impact on foam characteristics, Food Biophys. 11 (2016) 91–100.
[8] J. Liu, T. Henkel, Traditional Chinese medicine: are polyphenols and saponins the key ingredients triggering biological activities, Curr. Med. Chem. 9 (2002) 1483–1484.
[9] N. Fukada, H. Tanaka, Y. Shoyama, Isolation of the pharmacologically active saponin Ginsenoside Rb1 from Ginseng by immunoaffinity column chromatography, J. Nat. Prod. 62 (2000) 283–285.
[10] R. Brown, The natural way in cosmetics and skin care, Chem. Mark Rep. 254 (1998) FR8.
[11] C.R. Sitor, Aescin, pharmacology, pharmokinetics and therapeutic profile, Pharmacol. Res. 44 (2001) 183–193.
[12] R. Stanimirova, K. Marinova, S. Tcholakova, N.D. Denkov, S. Stoyanov, E. Pelan, Surface rheology of saponin adsorption layers, Langmuir 27 (2011) 12486–12498.
[13] K. Golemanov, S. Tcholakova, N. Denkov, E. Pelan, S.D. Stoyanov, Surface shear rheology of saponin adsorbed layers, Langmuir 28 (2012) 12071–12084.
[14] K. Golemanov, S. Tcholakova, N. Denkov, E. Pelan, S.D. Stoyanov, Remarkably high surface viscoelasticity of adsorbed layers of triterpenoid saponins, Soft Matter 9 (2013) 5738–5752.
[15] N. Pajuvera, S. Tcholakova, N. Denkov, E. Pelan, S.D. Stoyanov, Surface properties of adsorption layers formed from triterpendoid and steroid saponins, Coll. Surf. A 491 (2016) 18–28.
[16] J. Penfold, R.K. Thomas, I. Tucker, J.T. Petkov, S.D. Stoyanov, N. Denkov, K. Golemanov, S. Tcholakova, J.R.P. Webster, Saponin adsorption at the air-water interface – neutron reflectivity and surface tension study, Langmuir 34 (2018) 9540–9547.
[17] S. Tsibranska, A. Ivanova, S. Tcholakova, N. Denkov, Slef-assembly of escin molecules at the air-water interface studied by molecular dynamics, Langmuir 33 (2017) 8330–8341.
[18] K. Wojciechowski, M. Orcyzk, K. Marcinkowski, T. Kobiela, M. Trapp, T. Gutberlet, T. Geue, Effect of hydration of sugar groups on adsorption of Quillaja bark saponin at the air/water and Si/water interfaces, Coll. Surf. B 117 (2014) 60–67.
[19] S. Bottcher, S. Drusch, Interfacial properties of Saponin extracts and their impact upon foam characteristics, Food Biophys 11 (2016) 91–100.
[20] H. Jian, X. Liao, L. Zhu, W. Zhang, J. Jiang, Synergism and foaming properties in binary mixtures of a biosurfactant derived from Camellia Olefera Abel and synthetic surfactants, J. Coll. Int. Sci. 359 (2011) 487–492.
[21] K. Wojciechowska, M. Orczyk, T. Gutberlet, T. Geue, Complexation of phospholipids bt triterpene saponins in bulk and in a monolayer, Biochim. Biophys. Acta 1858 (2016) 363–373.
[22] C.I. Reichart, H. Salminen, C.N. Bonisch, C. Schaefer, J. Weiss, Concentration effect of Quillaja saponin-cosurfactant mixtures on emulfisfying properties, J. Coll. Int. Sci. 519 (2018) 71–81.
[23] S. Bottcher, M. Scampicchio, S. Drusch, Mixtures of saponins and β-lactoglobulin differ from classical protein/surfactant systems at the air-water interface, Coll. Surf. A 506 (2016) 765–773.
[24] K. Wojciechowski, M. Piotrowski, W. Popielarz, T.R. Sosnowski, Short and mid-term adsorption of Quillaja bark saponin and its mixtures with lysozyme, Food Hydrocolloids 75 (2011) 687–693.
[25] M. Piotrowski, J. Lewandowski, K. Wojciechowski, Biosurfactant-protein mixtures: Quillaja bark saponins at the air/water and oil/water interfaces in the presence of β-lactoglobulin, J. Phys. Chem. B 116 (2012) 4843–4850.
[26] A. Kezwon, K. Wojciechowski, Interaction of Quillaja bark saponins with food relevant proteins, Adv. Coll. Int. Sci. 209 (2014) 185–195.
[27] J.R. Lu, X. Zhao, M. Yaseen, Protein adsorption studied by neutron reflectivity, Curr. Opin. Coll. Int. Sci. 12 (2007) 9–16.
[28] M. Abe, J.F. Scamehorn (Eds.), Mixed Surfactant Systems, Surfactant Science Series, vol 124, 1995, Marcel Dekker, NY
[29] J.R. Lu, R.K. Thomas, J. Penfold, Surfactant layers at the air/water interface; structure and composition, Adv. Coll. Int. Sci. 84 (2000) 143–304.
[30] J. Penfold, R.K. Thomas, The limitations of models of surfactant mixing at interfaces as revealed by neutron scattering, PCCP 15 (2013) 7017–7027.
[31] P.X. Li, K. Ma, R.K. Thomas, J. Penfold, Analysis of the asymmetric synergy in the adsorption of zwitterionic – ionic surfactant mixtures at the air-water interface above and below the cmc, J Phys. Chem. B 129 (2016) 3677–3691.
[32] J. Penfold, E. Staples, L. Thompson, I. Tucker, The composition of nonionic surfactant mixtures at the air-water interface as determined by neutron reflectivity, Coll. Surf. 102 (1995) 127–132.
[33] M.L. Chen, J. Penfold, R.K. Thomas, T.J.P. Smythe, A. Perfumo, R. Marchant, I.M. Banat, P. Stevenson, A. Parry, I. Tucker, I. Grillo, Solution self-assembly and adsorption at the air-water interface of mono and dirhamnose rhamnolipids and their mixtures, Langmuir 26 (2010) 18281–18292.
[34] I.M. Tucker, A. Burley, S. Petkova, J. Penfold, R.K. Thomas, P.X. Li, J.R.P. Webster, R. Welbourne, Mixing of natural and synthetic surfactants: co-adsorption of saponins and sodium dodecyl sulfate at the air-water interface, Langmuir, 2020, submitted for publication.
[35] J. Penfold et al., recent advances in the study of chemical surfaces and interfaces by specular neutron reflection, J. Chem. Soc. Faraday Trans. 93 (1997) 3899–3917.
[36] J. Webster, S. Holt, R. Dalgleish, INTER: the chemical interfaces reflectometer on target station 2 at ISIS, Phys. B 385 (386) (2006) 1163–1166.
[37] J.R. Lu, Z.X. Li, R.K. Thomas, B.P. Binks, D. Crichton, P.D.I. Fletcher, J.R. MacNab, J. Penfold, The structure of monododecyl pentaethylene glycol monolayers with and without added dodecane at the air-solution interface, J. Phys. Chem. B 102 (1998) 5785–5793.
[38] N.M. van Os, J.R. Haak, L.A.M. Rupert, Phyisco-chemical properties of selected anionic, cationic and nonionic surfactants, Elsevier, Amsterdam, 1993.
[39] J.H. Clint, Micellisation of mixed nonionic surface active agents, J. Chem. Soc. Faraday Trans. 1 (71) (1975) 1327–1334.
[40] P.M. Holland, D.N. Rubingh, Nonideal multicomponent mixed micelle data, J. Phys. Chem. 87 (1983) 1984–1990.
[41] J. Liley, R.K. Thomas, J. Penfold, I.M. Tucker, J.T. Petkov, P. Stevenson, J.R.P. Webster, Surface adsorption in ternary surfactant mixtures above the cmc: the importance of the shape of the excess free energy of mixing, J. Phys. Chem. B 121 (2017) 2825–2838.
[42] J. Liley, R.K. Thomas, J. Penfold, I.M. Tucker, J.T. Petkov, P. Stevenson, J.R.P. Webster, The impact of electrolyte on the adsorption at the air-water interface from ternary surfactant mixtures above the cmc, Langmuir 33 (2017) 4301–4312.
[43] J. Liley, R.K. Thomas, J. Penfold, I.M. Tucker, J.T. Petkov, P. Stevenson, I. Banat, R. Marchant, M. Rudden, J.R.P. Webster, Adsorption at the air-water interface in biosurfactant-surfactant mixtures, Langmuir 33 (2017) 13027–13039.
[44] P.G. Nilsson, H. Wennerstrom, B. Lindman, Structure of micellar solutions of nonionic surfactants, nmr self-diffusion and proton relaxation studies of polyethylene oxide alkyl ethers, J. Phys. Chem. 87 (1983) 4756–4761.
[45] J. Penfold, I. Tucker, R.K. Thomas, E. Staples, R. Schuermann, Structure of mixed anionic/nonionic micelles: experimental observations relating to the role of headgroup electrostatic and steric effects and the effects of added electrolyte, J. Phys. Chem. B 109 (2005) 10760–10770.
[46] R. Zhang, P. Somasundaran, Abnormal micellar growth in sugar based and ethoxylated nonionic surfactants and their mixtures in dilute regimes using analytical ultracentrifigation, Langmur 20 (2004) 8552–8558.
[47] P.R. Majhi, K. Mukherjee, S.P. Moulik, S. Seu, N.P. Saku, Solution properties of a saponin in the presence of TritonX100 and Igepal, Langmuir 15 (1999) 6624–6630.
[48] K. Izutsu, S. Yoshioka, S. Kojima, T.W. Randolph, J.F. Carpenter, Effects of sugars and polymers on crystallisation of polyethylene glycol: phase separation between incompatible polymers, Pharm. Res. 9 (1996) 1393–2140.